Optics Letters

Optical spring tracking for enhancing quantum-limited interferometers

Scott Aronson,[1] Ronald Pagano,[1] Torrey Cullen,[2] Garrett D. Cole,[3] and Thomas Corbitt[1]

[1]*Louisiana State University Department of Physics & Astronomy, Baton Rouge, Louisiana 70803, USA*
[2]*LIGO Laboratory, California Institute of Technology, Pasadena, California 91125, USA*
[3]*Thorlabs Crystalline Solutions, Santa Barbara, California 93101, USA*

Modern interferometers such as LIGO have achieved sensitivities limited by quantum noise, comprising radiation pressure and shot noise. To mitigate this noise, a static system is employed that minimizes the quantum noise within the measurement band. However, since gravitational wave inspiral signals are a single frequency changing over time, only noise at the chirp frequency needs to be minimized. Here we demonstrate a proof-of-principle experiment of dynamically tracking a target signal using an optical spring, resulting in an increased signal-to-noise ratio (SNR). By injecting white noise to simulate excess shot noise, we found the SNR increased by up to a factor of 40 via dynamical tracking when compared to a static configuration.
© 2024 Optica Publishing

Introduction. Binary black hole and neutron star mergers are currently detected using laser interferometric observatories such as LIGO, Virgo, and KAGRA [1–4]. These gravitational wave signals are proportional to the time varying quadrupole moment of the merging system. As the separation distance between the two objects decreases due to the emission of gravitational waves (GWs), their rotational frequency and the resulting GW emission frequency increase in value until the merger. This increasing frequency is often referred to as the GW "chirp."

The LIGO and Virgo detectors have implemented higher power and frequency dependent squeezing to reduce their quantum noise [5,6]. Frequency dependent squeezing reduces shot noise above 100 Hz and reduces quantum radiation pressure noise (QRPN) [5]. This squeezing is focused on the region of the highest sensitivity, in the frequency range from 10 to 1000 Hz, and originates from the injection of squeezed vacuum into a filter cavity. This 300 m long cavity produces the desired frequency dependence by rotating the squeezing quadrature of the light.

In the current configuration, the quantum noise in LIGO is minimized around 100 Hz. This configuration is referred to as static, as the quantum noise is stationary with respect to time. With the future introduction of lower frequency band space-based GW detectors such as LISA [7], we may acquire knowledge of incoming signals to the ground-based detector

band with weeks to years of forewarning [8,9]. Using this prior information of an incoming GW signal, we show that it is possible to dynamically tune the quantum noise to be minimized over the range of the chirp.

The optical spring effect occurs when a cavity is operated off resonance, while having one or more mirrors susceptible to radiation pressure. The amount of circulating power and therefore radiation pressure depends on the total displacement from resonance. The optical field creates an effect analogous to a spring as the force from radiation pressure on the movable mirror is proportional to its position, similar to Hooke's law. By controlling the displacement from cavity resonance, the optical spring's resonant frequency can be actively controlled.

The use of an optical spring has been shown to provide different types of noise suppression [10–12]. In this Letter, we report a proof-of-principle experiment to dynamically control an optical spring [13] in order to track a target signal over time [14–16]. This dynamic tracking increases the SNR of the measurement when compared to a static configuration, improving the sensitivity by up to a factor of 40 in our experiment. For interferometer configurations such as LIGO, the optical spring effect can be achieved through the detuning of the signal recycling cavity (SRC) [9,17]. Currently, in the LIGO detectors, detuning between the SRC and the arm cavities creates an unintentional optical spring [18].

To understand the noise with the optical spring present, we start with an expression of the circulating power within the cavity [19]. This derivation assumes an instantaneous response of the circulating power in the cavity with changes in detuning.

$$P_c = \frac{P_0}{1 + \delta^2}. \tag{1}$$

The maximum on resonance circulating power is given by P_0, and the detuning δ is in units of linewidths of the cavity. The optical spring constant k_{OS} in the static limit is given by the following [20]:

$$k_{OS} = \frac{2}{c} \frac{dP_c}{dx} = \frac{2}{c} \frac{dP_c}{d\delta} \frac{d\delta}{dx}. \tag{2}$$

The displacement from resonance, x, can be written in terms of the detuning using the equations for cavity linewidth and the detuning of the cavity in units of the cavity linewidth [19]

resulting in the following:

$$x = \frac{\delta \lambda A}{8\pi}, \tag{3}$$

where A is the total losses within the cavity including the transmissivity of the mirrors and λ is the laser wavelength. This yields a final expression for k_{OS}:

$$k_{OS} = \frac{-32\pi\delta P_c}{\lambda c A (1 + \delta^2)}. \tag{4}$$

At the optical spring's resonant frequency mirror motion is amplified by the optical spring's quality factor, Q_{OS}, due to the blue-detuning of the laser. Q_{OS} results from the non-instantaneous response time of the cavity acting as a damping force resulting in a finite amplification of the mirror motion. It is beneficial to remove the effect of this amplification to recover the expected mirror motion without an optical spring present. In this "free-mass regime," the signal amplification from Q_{OS} is divided out, and any noise external to the cavity such as shot noise at the optical spring frequency is effectively suppressed.

The free-mass displacement fluctuations that arise due to radiation pressure shot noise is calculated by the following:

$$x_{rp} = \frac{1}{m\Omega^2} \frac{2P_c}{c} \sqrt{\frac{2hf}{P_{in}}}, \tag{5}$$

where Ω is the angular frequency, h is Planck's constant, P_{in} is the power incident on the cavity, c is the speed of light, and f is the laser frequency.

A standard reference for the performance of interferometric measurement devices is the standard quantum limit (SQL) [21]. This defines the minimum noise in the uncorrelated sum of the QRPN and shot noise. The SQL is not a hard limit however. It has been shown one method to achieve a measurement below the free-mass SQL is through the use of an optical spring [11].

To evaluate the performance at the optical spring frequency, we follow the derivation from [11]. First, we calculate the free-mass SQL via the following equation:

$$x_{SQL} = \sqrt{\frac{h}{\pi m \Omega^2}}. \tag{6}$$

We then set $\Omega = \Omega_{OS}$ and divide the radiation pressure x_{rp} by x_{SQL}. Here $\Omega_{OS} = \sqrt{\frac{k_{OS}+k_m}{m}}$, where k_m is the mechanical spring constant and m is the mass of the movable mirror. Since $k_m \ll k_{OS}$, we can approximate $\Omega_{OS} \approx \sqrt{\frac{k_{OS}}{m}}$.

By recalling k_{OS} from Eq. (4), we find the following:

$$\left.\frac{x_{rp}}{x_{SQL}}\right|_{\Omega_{OS}} = \frac{1}{c}\sqrt{\frac{32\pi hf P_c}{m\left(\sqrt{\frac{k_{OS}}{m}}\right)^2 A (1 + \delta^2)}}$$

$$= \sqrt{\frac{1}{-\delta}}. \tag{7}$$

The resulting noise level is predicted to be below the standard quantum limit for detunings less than -1 [11]. The above result is only valid for detunings $\delta < 0$ where a positive optical spring constant is present and Q_{OS} is sufficiently large. For $\delta > 0$, no optical spring resonance occurs and there is no suppression of the noise external to the cavity. Equation (7) predicts that as we
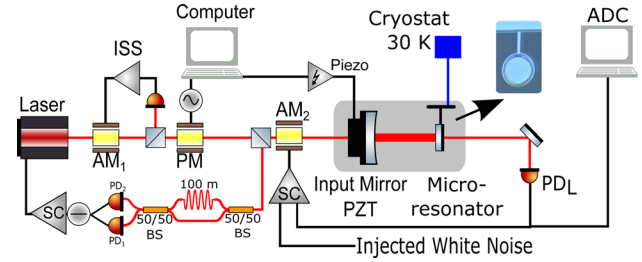

Fig. 1. Simplified experimental setup of optical spring tracking. The computer is used to inject a signal to the phase modulator (PM). The same computer also controls the detuning of the cavity via a piezo mount to track the signal frequency via a dynamically tunable optical spring. The servo controller (SC) stabilizes the cavity. White noise is injected into the SC to simulate shot noise.

sweep the optical spring to follow the target signal frequency, we surpass the SQL by a factor of $\sqrt{-\delta}$.

Experimental setup. The experimental setup for the optical spring tracking can be found in Fig. 1. The experiment consists of a 1064 nm Nd:YAG nonplanar ring oscillator (NPRO) laser. The laser intensity is actively stabilized via an intensity stabilization servo (ISS), and its frequency is controlled through a 100 m delay line interferometer.

The optical cavity is stored in a vacuum chamber at 10^{-8} Torr, and the micro-resonator is kept at cryogenic temperatures of around 30 K. The micro-resonator acting as the output mirror is an AlGaAs Bragg reflector with an effective mass of ~50 ng, supported by a thin GaAs cantilever [19]. The resonator has a fundamental mechanical resonance frequency of 876 Hz and quality factor, Q_m, of 25,000 ± 2200. The input stationary mirror has a radius of curvature of 1 cm and forms a stable cavity 1 cm in length. A seismic isolation platform suppresses all motion above 100 Hz by 50 dB [19]. For an optomechanical cavity to be dynamically stable, there must be a positive optical spring constant along with a positive damping coefficient [22,23]. In order to introduce a positive damping coefficient, an amplitude modulator (AM$_2$ in Fig. 1) is employed to stabilize the system.

A sinusoidal signal of varying frequency is injected into the laser beam via a phase modulator (PM). The signal to the PM was chosen to be constant in magnitude and linearly increase in frequency from 40 to 100 kHz over 10 s. The same computer that controls this signal injected to the phase modulator is also used to simultaneously vary the detuning of the cavity via a piezo mount on the input mirror. The piezo offset is calibrated in order to generate a desired detuning and thus optical spring frequency. To track the signal, the optical spring frequency is controlled to follow the frequency sent to the PM over time.

White noise is injected after PD$_L$ to simulate additional shot noise and enhance the effect of the optical spring noise suppression. Without this injection, the thermal noise contributions, which are above the SQL except for a small frequency band, would have obscured the final result. Therefore, the injected noise ensures the measurement is not limited by our particular setup, but rather the technique itself.

Four measurements were performed to show the performance of the optical spring tracking system. First, the detuning is swept with no signal present to determine the background. Then the detuning and the signal are swept together to establish a signal present over the background. To compare the performance to a static configuration, we fix the optical spring
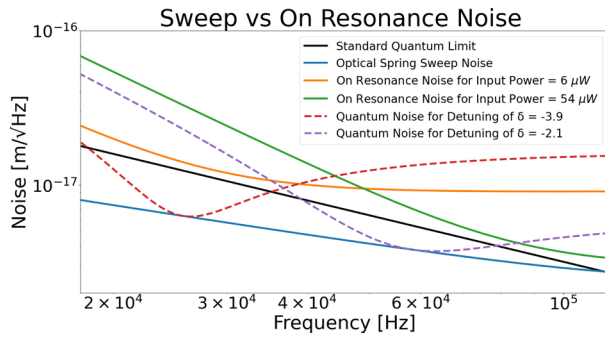
Fig. 2. Effective sweep noise compared to the SQL and the on resonance noise for two input powers. The sweep noise is predicted to be below the on resonance noise and is sub-SQL in the free-mass regime. The optical spring sweep noise curve is constructed from individual detuning curves (shown as dotted lines).

Fig. 3. Optical spring sweep noise curves compared to the modeled on resonance frequency dependent squeezing with 4.6 dB of output squeezing. The frequency dependent curves are a collection of the minimum noise as a function of input power. As optical losses are introduced, the frequency dependent measurements lose sensitivity. The optical spring sweep noise can be reduced through an increase in input power.

at 70 kHz and undertake the same procedure. The data is saved via an ADC at a 500 kHz sampling rate over 10 s. The time-series are then processed into a spectrogram and averaged in time using a moving average with a window of 100 samples to remove excess transient noise in the measurement.

Numerical simulations. In order to understand the total noise contributions of the system, we employ a numerical model utilizing the two-photon formalism [24]. This numerical simulation accounts for losses and the non-instantaneous response time of the cavity. For the purpose of this Letter, we neglect the contributions of classical noise sources such as thermal noise and focus solely on the intrinsic quantum noise of the system. Such quantum-limited interferometric systems have been demonstrated previously [11,25].

The key experimental parameters we feed into the model are the length of the cavity $L = 0.01$ m, the input power $P_{in} = 0.5$ mW, cavity losses of 220 ppm, a stationary input mirror of transmission $T_{in} = 50$ ppm, and a movable cantilever with $T_{out} = 450$ ppm and a mass of m = 50 ng. With these parameters, the cavity is dominated by radiation pressure below 100 kHz.

The code is then iterated over 100 detunings starting at a weak optical spring with $\delta = -5$ and ending with the maximum optical spring at $\delta = -\frac{1}{\sqrt{3}}$. For each detuning, the minimum in the quantum noise is recorded as "optical spring sweep noise." The resulting curve is plotted in Fig. 2. For modeled frequencies below 100 kHz, the sweep noise is lower than the free-mass SQL.

As the QRPN in our experimental setup is the dominant source of noise [25], operating the system on resonance in practice is nontrivial. For the experimental results discussed in the following section, we compare the noise at a single stationary optical spring frequency to the effective noise from sweeping the optical spring/detuning. The sweep noise is predicted to outperform the static configuration at all but a narrow band where the optical spring frequency sweep matched the static spring frequency.

The frequency dependent squeezing currently implemented in LIGO and Virgo is created by the injection of a squeezed vacuum state into the detector. Any optical losses contaminate the state through the introduction of unsqueezed vacuum [26]. Detectors must maintain very low optical losses to see the full benefit of squeezing. Optical spring tracking does not suffer from the same limitation of optical losses disrupting the measurement because the motion of the mirror is amplified. With frequency
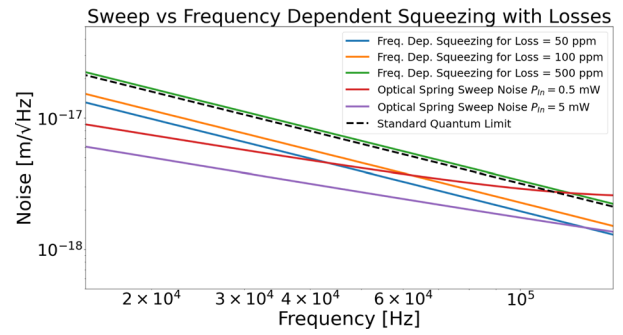
dependent squeezing, the motion remains constant, while the noise is reduced, which makes it more sensitive to losses. Figure 3 shows the effect of increased losses with frequency dependent squeezing compared to the optical spring sweep noise. Each frequency dependent squeezing curve is constructed from the minimum noise for each frequency when sweeping the input power.

Currently, in the LIGO interferometers, 17 dB of squeezing is generated, while the extrinsic optical losses result in just 4–5.8 dB of usable squeezing [5]. The minimum cavity loss of 50 ppm in Fig. 3 was chosen by modeling 17 dB of injected squeezing into our system and setting the loss such that the output squeezing of 4.6 dB was within the range of LIGO's measured squeezing. For cases where high optical losses cannot be avoided, optical spring tracking provides an alternative technique for quantum noise reduction. This method, unlike frequency dependent squeezing, does not require the use of a filter cavity.

Results. Using the background spectrogram and signal spectrogram, the SNR is calculated by evaluating the difference between the signal and the background and then dividing this difference by the background. With the SNR of both the sweep and static configurations calculated, they are then directly compared. For each time slice of the SNR spectrogram, the maximum value is recorded along the signal's frequency. This gives a measure of the signal extraction for each configuration as a function of frequency, as seen in Fig. 4. There is a clear increase in the SNR of the sweep configuration versus the static configuration for all frequencies except 70 kHz where the optical spring frequency sweep matched the static spring frequency.

Limitations of this technique include the need for prior knowledge of the time and morphology of an incoming signal. For our current implementation, there is also a limitation stemming from the bandwidth of the piezo response. In practice, something like an AOM or EOM could be implemented to directly modulate the laser frequency, granting more dynamic range.

The frequency range over which the optical spring can be easily positioned depends strongly on the configuration such as input power and detuning. So far, we have only considered the optomechanical resonance, but there is also an optical resonance. The optical resonance can also be controlled via the detuning and is higher in frequency than the optomechanical resonance. While the optomechanical resonance is more suited to measure
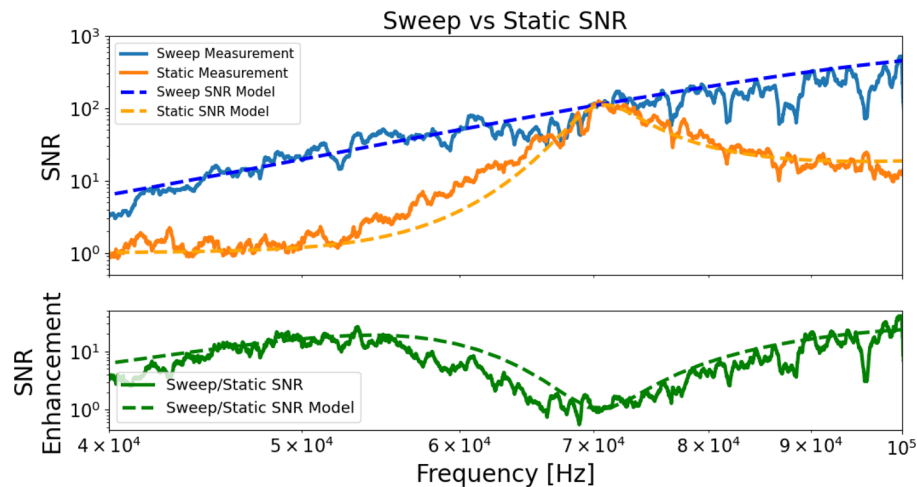
Fig. 4. Comparison of the injected signal SNR for sweep versus static configurations. The sweep configuration outperforms the static configuration for all but 70 kHz, where the optical spring frequencies were in proximity. The lower plot shows the ratio of the sweep SNR to the static configuration. The SNR enhancement has an average of 8.5 across the band, reaching a maximum value of 40.5 at 100 kHz.

earlier in a GW inspiral, the optical resonance may be used to broaden the measurement to frequencies up to and including binary black hole coalescence [9,27].

The optical spring control could be further enhanced by the introduction of optical parametric amplification [16,28]. This amplifier can modify the frequency of the optical spring providing an alternative method of tuning the resonator response.

Summary. We have predicted that by dynamically tracking the optical spring frequency to a known signal, a measurement can be performed with lower noise than on resonance cases and surpasses the free-mass standard quantum limit (SQL). When experimentally comparing the dynamic optical spring tracking to a static optical spring configuration, there is an average increase in the SNR by a factor of 8.5 with a maximal increase by a factor of 40 at 100 kHz.

Optical spring tracking can be utilized in any quantum-limited interferometric measurement system to measure a known signal changing in frequency over time. This method could serve as a complement [27] or an alternative to frequency dependent squeezing for systems, particularly those limited by optical losses. If desired, the method can track a single event, filtering out concurrent signals.

This technique could be used in the future for ground-based gravitational wave interferometers that have foreknowledge of a signal's arrival time and morphology. Such information may be ascertainable from planned projects such as LISA whose measurement band sits below LIGO. Improvements in interferometer sensitivity via dynamic detuning have also been proposed for third-generation detectors such as Cosmic Explorer [29].

Disclosures. The authors declare no conflicts of interest.

Data availability. Data underlying the results presented in this Letter are not publicly available at this time but may be obtained from the authors upon reasonable request.

REFERENCES

1. The LIGO Scientific Collaboration, J. Aasi, B. P. Abbott, R. Abbott, *et al.*, Class. Quantum Grav. **32**, 074001 (2015).
2. F. Acernese, M. Agathos, K. Agatsuma, *et al.*, Class. Quantum Grav. **32**, 024001 (2015).
3. K. Somiya (KAGRA Collaboration), Class. Quantum Grav. **29**, 124007 (2012).
4. B. P. Abbott, R. Abbott, T. D. Abbott, *et al.*, Phys. Rev. Lett. **116**, 061102 (2016).
5. D. Ganapathy, W. Jia, M. Nakano, *et al.*, Phys. Rev. X **13**, 041021 (2023).
6. F. Acernese, M. Agathos, A. Ain, *et al.*, Phys. Rev. Lett. **131**, 041403 (2023).
7. K. Danzmann, and the LISA study team, Class. Quantum Grav. **13**, A247 (1996).
8. A. Sesana, J. Phys.: Conf. Ser. **840**, 012018 (2017).
9. R. Tso, D. Gerosa, and Y. Chen, Phys. Rev. D **99**, 124043 (2019).
10. J. Cripe, T. Cullen, Y. Chen, *et al.*, Phys. Rev. X **10**, 031065 (2020).
11. T. Cullen, R. Pagano, J. Cripe, *et al.*, Phys. Rev. Lett. **133**, 113602 (2024).
12. T. Cullen, S. Aronson, R. Pagano, *et al.*, Opt. Lett. **47**, 2746 (2022).
13. B. S. Sheard, M. B. Gray, C. M. Mow-Lowry, *et al.*, Phys. Rev. A **69**, 051801 (2004).
14. B. J. Meers, A. Krolak, and J. A. Lobo, Phys. Rev. D **47**, 2184 (1993).
15. D. A. Simakov, Phys. Rev. D **90**, 102003 (2014).
16. J. Zhang, H. Sun, H. Guo, *et al.*, Appl. Phys. Lett. **122**, 261106 (2023).
17. A. Buonanno and Y. Chen, Class. Quantum Grav. **19**, 1569 (2002).
18. L. Sun, E. Goetz, J. S. Kissel, *et al.*, Class. Quantum Grav. **37**, 225008 (2020).
19. J. Cripe, "Broadband measurement and reduction of quantum radiation pressure noise in the audio band," Ph.D. thesis (Louisiana State University, 2018).
20. T. Corbitt, "Quantum noise and radiation pressure effects in high power optical interferometers," Ph.D. thesis (Massachusetts Institute of Technology, 2008).
21. V. B. Braginsky, Y. I. Vorontsov, and K. S. Thorne, Science **209**, 547 (1980).
22. R. Singh, G. D. Cole, J. Cripe, *et al.*, Phys. Rev. Lett. **117**, 213604 (2016).
23. T. Corbitt, Y. Chen, E. Innerhofer, *et al.*, Phys. Rev. Lett. **98**, 150802 (2007).
24. T. Corbitt, Y. Chen, and N. Mavalvala, Phys. Rev. A **72**, 013818 (2005).
25. J. Cripe, N. Aggarwal, R. Lanza, *et al.*, Nature **568**, 364 (2019).
26. L. McCuller, C. Whittle, D. Ganapathy, *et al.*, Phys. Rev. Lett. **124**, 171102 (2020).
27. J. Harms, Y. Chen, S. Chelkowski, *et al.*, Phys. Rev. D **68**, 042001 (2003).
28. M. Korobko, F. Khalili, and R. Schnabel, Phys. Lett. A **382**, 2238 (2018).
29. V. Srivastava, D. Davis, K. Kuns, *et al.*, Astrophys. J. **931**, 22 (2022).